ICAS 2021 SHANG HAI
32nd Congress of the International Council of the Aeronautical Sciences
September 6-10, 2021 Pudong Shangri-La, Shanghai, China

Experimental study on critical heat flux characteristics of R134a flow boiling in a horizontal 2.1 mm tube under hypergravity

Jianjun Han[1], Gen Li[2]

[1]Nanjing engineering Institute of Aircraft System, Jincheng, AVIC,33 Shuige St, Nanjing 210000, China
[2]Key Laboratory of Aircraft Environment Control and Life Support, MIIT, Nanjing University of Aeronautics and Astronautics, 29 Yudao St., Nanjing 210016, China.

Abstract

An experimental study on critical heat flux (CHF) of R134a flow boiling in a 2.1 mm inner diameter (ID) horizontal copper tube under different hypergravity is conducted. The experimental range of parameters is gravity levels of normal gravity (1g) and hypergravity (1.41g–3.16g), mass fluxes of 614, 395 and 294 kg/m^{2}s, saturation pressures of 0.628 and 0.562 MPa, and inlet vapor qualities from 0.05 to 0.375. Based on the experimental data, the effects of different gravity, inlet vapor quality, mass flux, and saturation pressure on the CHFs were analyzed, the results show that the CHFs of R134a decrease with increasing gravity levels at high mass flux, while the CHFs decrease with increasing gravity levels only at inlet vapor quality larger than 0.2 at other lower mass flux. In addition, the CHFs decrease with increasing inlet vapor quality under different gravity levels, mass flux, and saturation pressure. The effects of saturation pressure on the CHFs are inapparent, while the effects of mass flux are significant, and this main because the mean vapor quality of test section decrease with increasing mass flux, thus the CHFs are higher than that under low mass flux.

Keywords: Flow boiling, critical heat flux, micro/mini-channel, hypergravity, R134a

1. Introduction

Accurate prediction of micro/mini-channel critical heat flux (CHF) is very important for design of modern flight vehicles such as fifth generation jet fighter (F-35, J-20) and large passenger aircraft (A-380, Boeing 787), etc., and it could cause a drastic reduction of heat transfer coefficient (HTC) when CHF occurs. As the HTC decreasing sharply, the wall temperature of tube increases abruptly, that causes the material of heated facilities destroyed, consequently, which is called boiling crisis[1]. Because some flight vehicles often perform hypergravity maneuvers, it is necessary to investigate the flow boiling CHF characteristics in mini/micro-channels under hypergravity [2].

According to mechanistic analysis, the CHF is roughly classified as two types, DNB (departure from nucleate boiling) CHF and dry-out CHF[3], as depicted in Fig 1. They are based on the different explanations for the trigger mechanism of CHF under different conditions. The DNB type CHF usually occurs where bubbles grow too fast to depart from heated surface due to very high heat flux. In this case, the temperature of bulk flow is lower than or equal to the saturated temperature. Actually, most of DNB CHF takes place in subcooling boiling conditions because of the existence of gas-phase (bubbles) between heated surface and cooling fluid, which awfully weakens the boiling heat transfer capability. The inducement for dry-out type CHF, just as its name implies, is mainly the avulsion and dry-out of liquid film caused by flow blowing and heat braising. The dry-out CHF usually occurs in annular flow pattern where the central core flow has a high velocity and can easily disperse the thin liquid film with help of the hot surface of tube wall. The DNB CHF works under much higher heat flux than the dry-out CHF, but both of them should be paid attention to in practical conditions related to the efficiency and security of operating heated equipment[4-6].

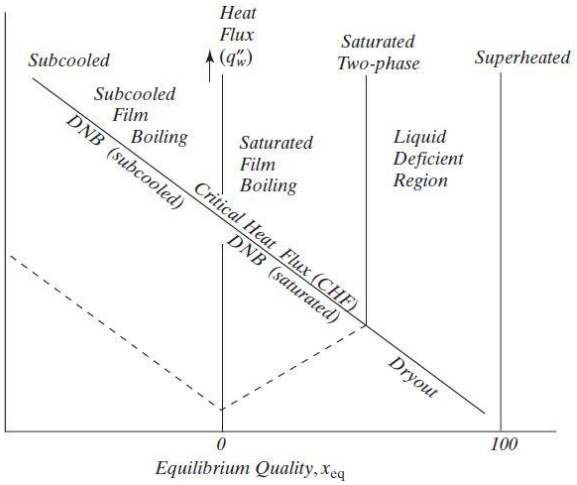

Figure 1 –Qualitative depiction of the flow boiling map and critical heat flux

Kim et al.[7] conducted experiments for the vertical orientation under outlet pressures of 13, 16.5, and 23.9 bar, mass fluxes of 285–1300 kg/m^{2}s and inlet subcooling temperatures of 5–40℃ in the R134a CHF test loop. The results showed that the CHF in the rifled tube was enhanced to 40–60% for the CHF in the smooth tube with depending on the rifled geometry and flow parameters such as pressure and mass flux. Haas et al.[8] investigated critical heat flux for flow boiling of water at low pressures on technically smooth surface tubes. The experiments were performed in a vertical annular test section of two coaxial tubes, and the inner Zircaloy-4 tube with an outer diameter of 9.5 mm was directly heated over a length of 326 mm. The experimental parameters of inlet subcooling enthalpy, outlet pressure and mass flux were varied in the ranges of 100–250 kJ/kg, 115–300 kPa, and 250–1000 kg/m^{2}s. They concluded that the CHF values were almost constant for pressures between 120 and 200 kPa, and showed an increasing tendency for pressures between 200 and 300 kPa for constant mass flux and inlet conditions. Ali and Palm[9] carried out experiments in vertical circular mini-channels with internal diameters of 1.22 mm and 1.70 mm and a fixed heated length of 220 mm. They used R134a as working fluid. Mass flux was varied from 50 kg/m2 s to 600 kg/m^{2}s and experiments were performed at two different system pressures corresponding to saturation temperatures of 27 ℃ and 32 ℃. Experimental results showed that the dry-out heat flux increased with mass flux and decreased with tube diameter while system pressure had no clear effect for the range of experimental conditions covered. Qu and Mudawar[10] measured CHF for a water-cooled micro-channel heat sink containing 21 parallel 215×821 μm channels. Tests were performed with deionized water over a mass velocity range of 86–368 kg/m^{2}s, inlet temperatures of 30 and 60 ℃, at an outlet pressure of 1.13 bar. They founded that CHF in mini/micro-channel heat sinks increased with increasing mass velocity but, because of the loss of subcooling due to the backward vapor flow, CHF was virtually independent of inlet temperature. This was a fundamental departure of mini/micro-channel heat sink behavior from that of single mini-channels. Mauro et al.[11] studied an extensive experimental campaign for the measurement of saturated CHF in a multi-microchannel copper heat sink. The base critical heat flux was measured using three HFC Refrigerants (R134a, R236fa and R245fa) for mass fluxes ranging from 250 to 1500 kg/m^{2}s, inlet subcooling from -25 to -5 K and saturation temperatures from 20 to 50 ℃. The analysis showed that significantly higher CHF was obtainable with the split flow system (one inlet–two outlets) compared to the single inlet–single outlet system, providing also a much lower pressure drop. Wojtan et al.[12] performed a series of tests to determine the saturated CHF in 0.5 mm and 0.8 mm internal diameter micro-channel tubes as a function of refrigerant mass velocity, heated length, saturation temperature and inlet liquid subcooling. The working fluid was R134a and R245fa. The results show a strong dependence of CHF on mass velocity, heated length and microchannel diameter but no influence of liquid subcooling (2–15 ℃) was observed.

An overview of the previous work shows that studies on the CHFs are mainly conducted under normal gravity (1g), and few literatures reported under hypergravity. This paper presents an experimental study on flow boiling CHF of R134a in a 2.1 mm horizontal smooth tube under hypergravity levels by using a centrifugal machine on the ground. In addition, the experimental data are compared among different gravity levels, inlet vapor qualities, mass fluxes and saturation pressures.

2. Experimental apparatus and procedure

2.1 Experimental setup

The experimental setup for investigating the critical heat flux of saturated flow boiling under hypergravity is composed of a centrifugal acceleration machine, a refrigerant loop, and a measure-control system.

The centrifugal acceleration machine consists of a turntable, two electric brushes and a motor, as shown in Fig. 2. The turntable provided the required centripetal acceleration to simulate the hypergravity environment by adjusting the electrical frequency of the motor, and the power used by the equipment on the turntable was supplied through the electric brushes during the experiment.

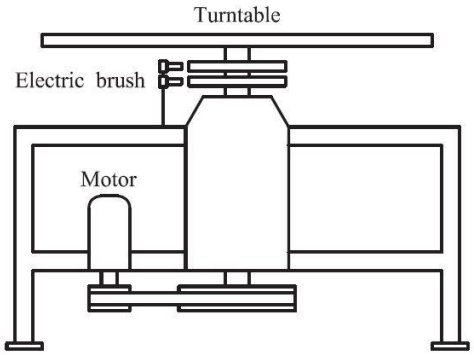

Figure 2 –Schematic and reality image of the centrifugal acceleration machine

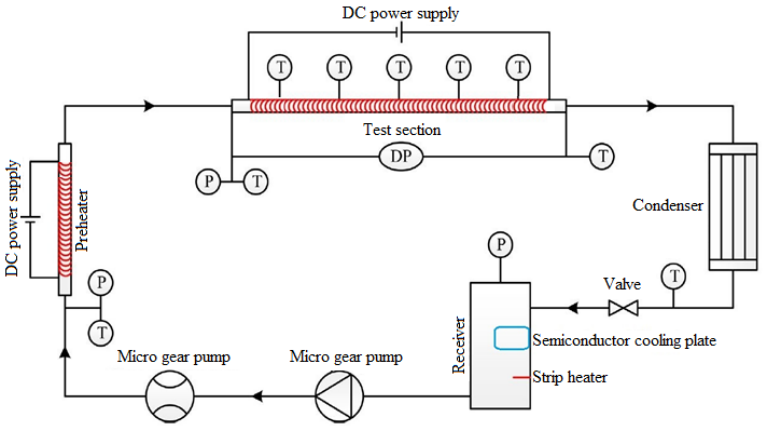

Figure 3 –Schematic of the refrigerant loop

The refrigerant loop consisted of a preheater, test section, condenser, micro gear pump, micro flow meter, strip heater, and a receiver with semiconductor cooling plate, as shown in Fig. 3. The liquid refrigerant R134a in the receiver is pumped by the micro gear pump. Then, it passes through the micro flow meter, entering the preheater, where it is heated to a saturation boiling state with a preset vapor quality by adjusting the preheater DC supply power. The saturated two-phase refrigerant from the preheater passes through the developing section and flows into the test section, where it is heated to a required outlet quality by adjusting the DC power supplied to the test section. Flowing out the test section, the refrigerant is directed to the condenser, where it is condensed and sub-cooled by exchanging heat with the ice-liquid water, and then returns back to the receiver. In this way, the refrigerant circulates in the experimental loop ceaselessly.

The test section was made of a 200 mm long straight copper tube with an ID of 2.1 mm and an outer diameter (OD) of 4 mm. The test section was wound uniformly with an enameled Ni-Cr wire as the heating device, which was connected with the DC power supply, and then was covered with insulation materials, as shown in Fig. 4. The preheater was made of the same copper tube and had the heating device made of the same way as the test section. The receiver outside surface was mounted with the strip heater and semiconductor cooling plate controlled by electrical power to keep the system pressure stable. In order to eliminate the entrance effect, immediately preceding the test section is a 0.1 m long straight developing section made of the same copper tube as the test section. All the tubes and containers in the refrigerant loop were well insulated, and all the tube connections had smooth interfaces to avoid the interference with the flow patterns. The refrigerant flow rate was regulated by the frequency inverter of the pump. Four T-type thermocouples were fixed evenly along

the test section, and two on the inlet and outlet tube wall of the preheater to measure the outer wall temperature.

The test section was horizontally fixed on the turntable with a distance of 0.9 m to the central axis, the flow direction of the refrigerant in the test section is from the right to the left, and the turntable rotates anti-clockwise, as shown in Fig. 5. This arrangement ensures the same centripetal acceleration vectors perpendicular to the test section, i.e. the centripetal acceleration vectors perpendicular to the test section keep constant along the flow direction.

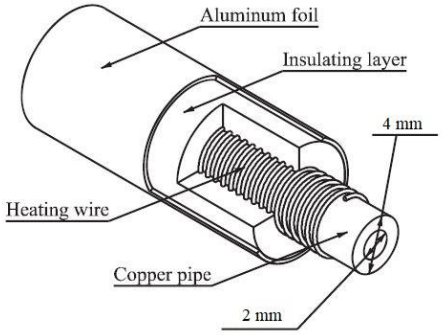

Figure 4 –Schematic of the test section

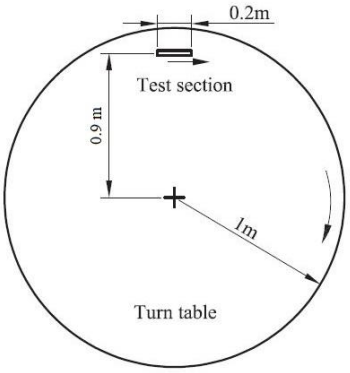

Figure 5 –Location of the test section in the turn table

2.2 Experimental procedure

At first, the centrifugal acceleration machine was set in stationary state, while the mass flow rate, saturation pressure, heating power of the test section and heating power of the pre-heater were regulated to the desired values when a steady state was reached. Then, the centrifugal acceleration was successively regulated from 0 to 3 g with an interval of 1 g by regulating the rotational speed of the centrifugal acceleration machine, while keeping the mass flow rate, saturation pressure, heating power of the test section, and heating power of the pre-heater constant. The data were taken every time the steady state was reached, and thus the experimental data under different gravity levels were obtained.

3. Data reduction

3.1 Centripetal acceleration and hypergravity

Since the test section length *L* (200 mm) is much shorter than the arm length L_a (900 mm), the distance between the middle of the test section and the central axis of the turntable, the centripetal acceleration in the middle of the test section can be used to represent that of the whole test section. Therefore, the centripetal acceleration of the test section $a_c$was calculated by

$$a_c = (2\pi n)^2 L_a \tag{1}$$

The hypergravity a_h is the resultant of the centripetal acceleration a_c and Earth's gravity (1 g), which was determined by

$$a_h = \sqrt{{a_c}^2 + g^2} = g\sqrt{(a_c/g)^2 + 1} \tag{2}$$

When the rotational speed $\mathrm{n} = 0$, $a_c = 0$ and $a_h = 1\ g$, meaning that the refrigerant flow is under Earth's gravity. On the other hand, when $\mathrm{n} > 0$, $a_c > 0$ and $a_c/g > 0$ so that $a_h > 1g$, meaning that the refrigerant flow is under hypergravity.

3.2 Saturation pressure

The refrigerant is in saturated state before entering the test section, thus the saturation pressure of the test section p is determined by

$$p = p_m - \frac{1}{2}\Delta p \tag{3}$$

where p_m is the inlet pressure and Δp is the pressure drop of the test section. When knowing p, the saturation temperature of the refrigerant in the test section can be obtained by using NIST's software REFPROP.

3.3 Vapor quality

The vapor quality was determined using the energy balance method. Since the outlet of the pre-heater is the inlet of the test section, the inlet vapor quality of the test section $x_{in}$was calculated by

$$x_{in} = \frac{1}{h_{ig,in}}\left(\frac{Q_{pre}}{m} - \Delta h_{l,per}\right) \tag{4}$$

where $h_{ig,in}$ is the latent heat of vaporization of the refrigerant at the inlet of the test section, $\Delta h_{l,per}$is the liquid enthalpy difference between the outlet and the inlet of the preheater, m is the mass flow rate, and Q_{pre} is the net heating power of the pre-heater.

Similarly, the outlet vapor quality of the test section was calculated by

$$x_{out} = x_{in} + \frac{Q_{test}}{m h_{ig,out}} \tag{5}$$

where $h_{ig,out}$is the latent heat of vaporization of the refrigerant at the outlet of the test section. Q_{test} is the net heating power of the test section. The average vapor quality of the test section was obtained by taking the arithmetic mean value of the inlet and outlet vapor qualities:

$$x = \frac{1}{2}(x_{in} + x_{out}) \tag{6}$$

3.4 Heat flux

The heat flux of the test section is calculated by

$$q = \frac{Q_{test}}{A_{heat}} \tag{7}$$

Where $A_{heat}$is the heating area of the test section.

4. Uncertainty and reliability validation

4.1 Uncertainty

Each thermocouple used in the present experiment was calibrated by using a high precision calibration bath with an accuracy of 0.1 °C. The mass fluxes were measured by a micro flow meter, which had a measuring range of 5–1000 ml/min with an accuracy of ±0.5% full scale (FS), and the micro flow meter was installed near the center of the turntable to reduce the interferences from the vibration and centrifugal force. Two pressure transmitters having a measuring range of 0–1 MPa and an accuracy of 0.5% FS were used to measure the inlet relative pressures of both the test section and the preheater, and the inlet absolute pressures of the test section and preheater were calculated by adding the inlet relative pressures and the ambient pressure measured by an aneroid barometer, which had an accuracy of ±100 Pa. The experimental uncertainties of measured and calculated parameters, including diameter, length, temperature, mass flow rate, relative pressure, heat flux, vapor quality, rotating speed and hypergravity were summarized in Table 1.

Table 1 –Uncertainties of measured and calculated parameters

Parameter	Uncertainty
Tube diameter	± 10 μm
Tube length	± 1 mm
Temperature	± 0.1 ℃
Mass flow rate	± 0.5% FS
Relative pressure	± 0.5% FS
Ambient pressure	± 100 Pa

Parameter	Uncertainty
Heat flux	± 1.37 %
Rotating speed	± 0.2 %
Hypergravity	± 0.42 %

4.2 Reliability validation

The reliability of the experimental setup was validated through the single-phase heat transfer experiments under Earth's gravity. The experimental single-phase Nusselt number was compared with the Gnielinski[13] correlation to validate the experimental system. One of the results is illustrated in Fig. 6, which shows that the measurements of the single-phase Nusselt number agrees well with the predictions of the Gnielinski correlation, indicating that the experimental setup for CHF of R134a was reliable.

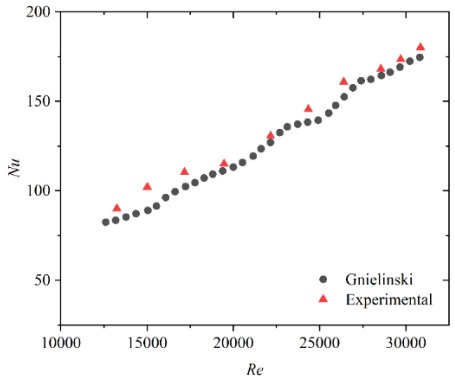

Figure 6 –Comparison of the single-phase Nusselt number

5. Experimental results and discussion

The experimental conditions of the R134a saturated flow boiling CHF were the gravity levels of 1g (Earth's gravity) 1.41g, 2.24g, and 3.16g, mass fluxes of 614, 395 and 294 kg/m^{2}s, saturation pressures of 0.628 and 0.562 MPa, and inlet vapor qualities from 0.05 to 0.375, as shown in the Table 2.

Table 2 Experimental conditions under different gravity levels

G (kg/m^{2}s)	p (MPa)	a_c	a_h
614, 395, 294	0.628,0.562	0 g	1 g
614, 395, 294	0.628,0.562	1 g	1.41 g
614, 395, 294	0.628,0.562	2 g	2.24 g
614, 395, 294	0.628,0.562	3 g	3.16 g

The experimental results of the CHF under three hypergravity levels (1.41g, 2.24g, and 3.16g) and normal gravity (1g) are illustrated in Fig. 7, where the normal gravity data are included to facilitate the comparison of the different gravity effects.

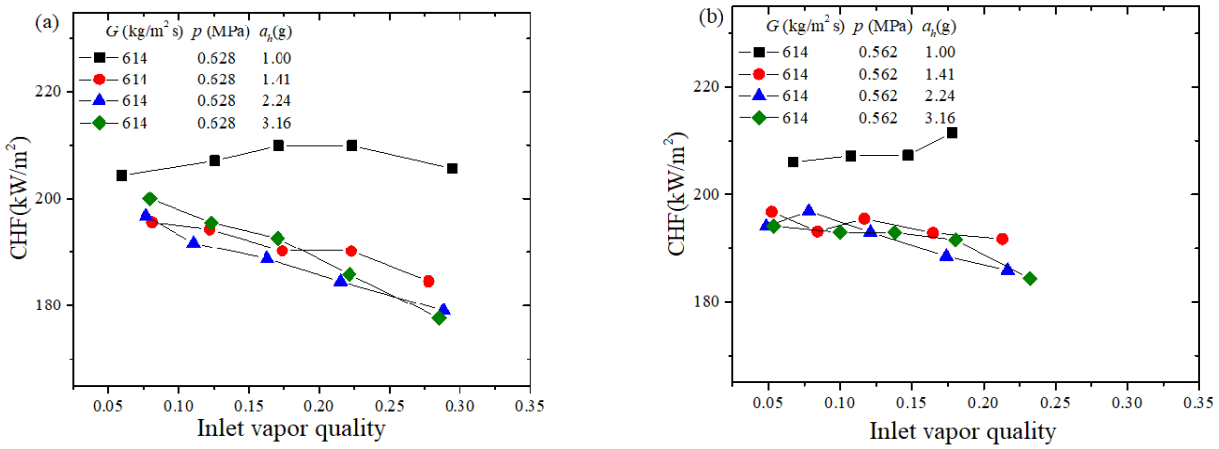

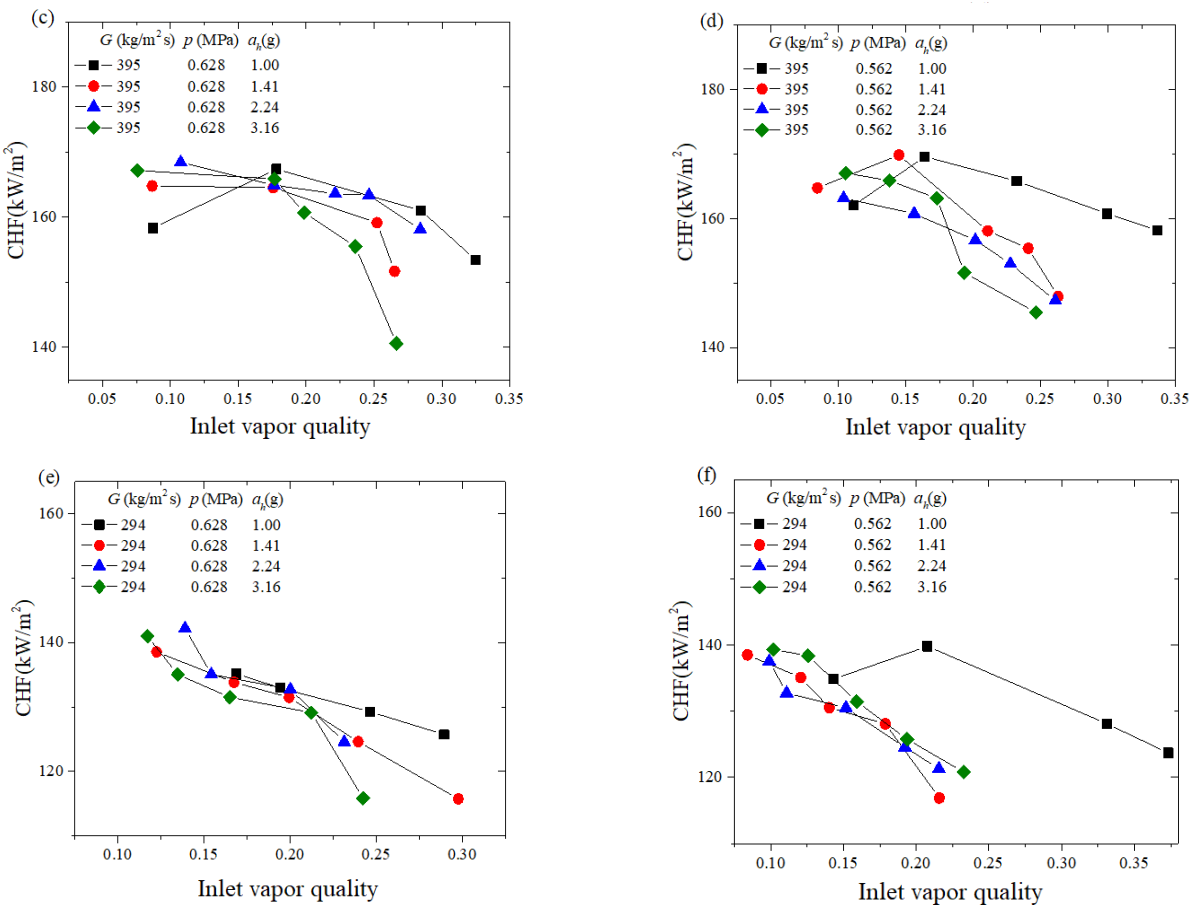

Figure 7 –Flow boiling CHF under different gravity levels

From Fig.7, the following points can be seen:

(1) The CHFs of R134a decrease with increasing gravity levels for whole range of inlet vapor quality at conditions of G = 614 kg/m^{2}s (Fig. 7a, Fig. 7b), while at other two mass flux conditions G = 395 and 294 kg/m^{2}s, the CHFs decrease with increasing gravity levels only at inlet vapor quality larger than 0.2. Therefore, the conclusion can be gained that the effects of gravity levels are more significant at high mass flux than that at low mass flux.

(2) The trends of the CHF variation with inlet vapor quality under different gravity levels, mass flux, and pressure are similar to each other, all decrease evidently with increasing inlet vapor quality. The main reason is that more inlet vapor quality lead to more vapor quality of test section, and the more vapor quality is, the higher gas volume fraction is, which could cause dry-out occurs more easily.

(3) The effects of saturation pressure on the CHFs are inapparent through Fig. 7 (a) and (b), Fig. 7 (c) and (d), Fig. 7 (e) and (f), and the CHF increase with increasing mass flux obviously, as can be seen from Fig. 7 (a), (c) and (e). One reason that the enhancement of increasing saturation pressure on the CHFs is indistinct due to the pressure difference of the experiments is small, the high pressure is 0.628 MPa, and the lower one is 0.562 MPa, just a little bit more than 11% of difference. Higher mass fluxes lead to higher CHFs mainly because that at the same inlet vapor quality and saturation pressure, the mean vapor quality of test section decrease with increasing mass flux, thus the CHFs are higher than that under low mass flux.

6. Conclusions

A series of experiments on the two-phase flow boiling CHF of R134a in a horizontal 2.1 mm tube under normal gravity (1g) and hypergravity levels (1.41g–3.16g) were conducted, with mass fluxes of 614, 395 and 294 kg/m^{2}s, saturation pressures of 0.628 and 0.562 MPa, and inlet vapor qualities from 0.05 to 0.375. With the experimental data, the effects of the gravity level, inlet vapor quality, mass flux, and saturation pressure on the CHFs were analyzed, the conclusions are summarized

below.

(1) The CHFs of R134a decrease with increasing gravity levels at high mass flux, while the CHFs decrease with increasing gravity levels only at inlet vapor quality larger than 0.2 at other lower mass flux.

(2) The CHFs decrease evidently with increasing inlet vapor quality under different gravity levels, mass flux, and saturation pressure, and the trends are similar to each other.

(3) The effects of saturation pressure on the CHFs are inapparent, while the effects of mass flux are significant, this main because the mean vapor quality of test section decrease with increasing mass flux, thus the CHFs are higher than that under low mass flux.

7. Contact Author Email Address

Mailto: 270473491@qq.com

8. Copyright Statement

References

[1] Ong C L, Thome J R. Macro-to-microchannel transition in two-phase flow: Part 2-Flow boiling heat transfer and critical heat flux. *Experimental Thermal & Fluid Science*, 2011, 35(6): 873-886.

[2] Li G, Fang X, Tang D, Luo Z, Chen Y. Experimental study on saturated flow boiling heat transfer of R1234yf in a horizontal 2.01 mm tube under hypergravity. *International Journal of Refrigeration*, 2021, 127: 12-20.

[3] Roach G M, Jr, Abdel-Khalik S I, Ghiaasiaan S M. Low-Flow Critical Heat Flux in Heated Microchannels. Nuclear science and engineering: *the journal of the American Nuclear Society*, 1999, 131(2): 411-425

[4] Stoddard R M, Blasick A M, Ghiaasiaan S M. Onset of flow instability and critical heat flux in thin horizontal annuli. *Experimental Thermal and Fluid Science*, 2002.

[5] Qi S L, Zhang P, Wang R Z. Flow boiling of liquid nitrogen in micro-tubes: Part II-Heat transfer characteristics and critical heat flux. *International Journal of Heat and Mass Transfer*, 2007, 50(25-26): 5017-5030.

[6] Shibahara M, Fukuda K, Liu Q S. Correlation of high critical heat flux during flow boiling for water in a small tube at various subcooled conditions. *International Communications in Heat and Mass Transfer*, 2017, 82: 74-80.

[7] Kim C H, Bang I C, Chang S H. Critical heat flux performance for flow boiling of R-134a in vertical uniformly heated smooth tube and rifled tubes. *International Journal of Heat and Mass Transfer*, 2005, 48(14): 2868-2877.

[8] Haas C, Schulenberg T, Wetzel T. Critical heat flux for flow boiling of water at low pressure in vertical internally heated annuli. *International Journal of Heat and Mass Transfer*, 2013, 60: 380-391.

[9] Ali R, Palm B. Dryout characteristics during flow boiling of R134a in vertical circular minichannels. *International Journal of Heat and Mass Transfer*, 2011, 54(11-12): 2434-2445.

[10]Qu W, Mudawar I. Measurement and correlation of critical heat flux in two-phase micro-channel heat sinks. *International Journal of Heat and Mass Transfer*, 2004, 47(10-11): 2045-2059.

[11][Mauro A W, Thome J R, Toto D. Saturated critical heat flux in a multi-microchannel heat sink fed by a split flow system. *Experimental Thermal & Fluid Science*, 2010, 34(1): 81-92.

[12]Wojtan L, Rémi Revellin, Thome J R. Investigation of saturated critical heat flux in a single, uniformly heated microchannel. *Experimental Thermal & Fluid Science*, 2006, 30(8): 765-774.

[13][Gnielinski V. New equations for heat and mass transfer in turbulent pipe and channel flow, *International Chemical Engineering* 1976, 16: 359–368.